https://doi.org/10.15407/ujpe71.1.3

MAYADA J. AL-SHARAA,[1] HASHIM YOUSEF YAQOUB AL-KAZRAJY,[2]
QASSIM SHAMKHI AL KHAFAJI,[3] SHAYMAA AWAD KADHIM[3]

[1] Department of Physics, College of Science, University Misan
(Maysan, Iraq; e-mail: mayadajassim@uomisan.edu.iq)
[2] Department of Physics, College of Science, University of Thi-Qar
(Nasiriyah, Thi Qar Governorate, Iraq)
[3] Department of Physics, Faculty of Science, University of Kufa
(P.O Box 21, Kufa, Najaf Governorate, Iraq)

CALCULATION OF THE HARTREE–FOCK ENERGIES FOR p-TYPE SHELLS OF SOME NEGATIVE IONS

The energies of the subshells (2p, 3p) and selected atomic properties of several negative ions ($S^{(-1)}$, $Cl^{(-1)}$, $K^{(-1)}$, and $Sc^{(-1)}$) were calculated within the Hartree–Fock approximation. The energies were evaluated for the atomic number $16 \leq Z < 21$. The study showed that the estimates used to calculate the atomic properties using this method were accurate. The functions $D(r_1)$ and $f(r_{12})$, which describe the probability of finding a single electron and two electrons separated by a distance r_{12}, respectively, were studied, and the values of the Hartree–Fock expectations $\langle r_{12}^n\rangle, \langle r_1^n\rangle$ were studied, where n is the value between –2 to 2. The expected energy value is $\langle E_{HF}\rangle, \langle V_T\rangle, \langle V_{en}\rangle, \langle V_{ee}\rangle$ and $\langle T\rangle$ were calculated. We can conclude that the increasing of an atomic number leads to the increasing of all the studied energies of the elements under consideration. All functions were standard. The Mathcad 2014 application was used to program the equations. Regarding the computations, they were all done in atomic units (a.u).

Keywords: Schrödinger equation, atomic properties, negative ion, Hartree–Fock energies.

1. Introduction

Quantum mechanics can be represented in many ways, but the most common formulation is the Schrödinger equation, to which the basic equations of all quantum mechanical systems are governed. In the simple case of time-independent systems, the Schrödinger equation is given as follows [1, 2]

$$\hat{H}\Psi = E\Psi, \tag{1}$$

where E is the energy, $\hat{H}$ is the Hamiltonian, and ψ is the wave function. In general, the Hamiltonian factor consists of

$$\hat{H} = -\frac{\hbar^2}{2m_e}\sum_{i=1}^{N}\nabla_i^2 - \sum_{i=1}^{N}\frac{Ze^2}{r_i} + \sum_{i=1}^{N}\sum_{j>i}^{N}\frac{e^2}{r_{ij}}. \tag{2}$$

The Schrödinger equation has been solved for many simple systems such as the hydrogen atom system and hydrogen-like atoms, which allows for a complete treatment of the electronic structure of the hydrogen atom and hydrogen-like atoms through the complete and accurate solution of the Schrödinger equation and obtaining wave functions describing these systems from these solutions, but such success cannot be easily achieved for any atom other than the hydrogen atom or atoms similar to it, because when

---

Citation: AL-Sharaa M.J., Al-Kazrajy H.Yo.Ya., Al Khafaji Q.Sh., Kadhim Sh.A. Calculation of the Hartree–Fock energies for p-type shells of some negative ions. *Ukr. J. Phys.* **71**, No. 1, 3 (2026). https://doi.org/10.15407/ujpe71.1.3.

there is more than one electron around the nucleus, this causes the emergence of new forces, which are the repulsive forces between electrons, which results in an interaction energy inversely proportional to the distance between the two electrons [3, 4].

Therefore, it is necessary to use approximation techniques to make the problem solvable. At this point, it becomes essential to understand the underlying mechanics of the problem. If important conclusions are to be drawn from the process of solving the problem, suitable approximations must be employed. Among these approximations, the oldest and most fundamental one is attributed to Hartree, who postulated that the total wave function $\psi(r_1, r_2, ..., r_N)$ for N electrons can be found by multiplying the wave functions of a single particle [5, 6]

$$\psi(r_1, r_2, ..., r_N) = \varphi_1(r_1)\varphi_2(r_2), ..., \varphi_N(r_N) = \\ = \prod_{N=1}^{i} \varphi_i(r_i), \tag{3}$$

where $\varphi_i(r_i)$ depends on the coordinates r_i and the spin of the electron. Since there is more than one electron, each of them must move independently of the others according to Eq. (3), which states that each electron moves within the average electrostatic potential of the rest of the electrons. Equation (3) represents the Hartree product, which provides a mean-field approximation but does not satisfy the antisymmetry requirement for fermionic wave functions and therefore cannot serve as the complete electronic wave function. This occurs as a result of electron-electron interactions being incorrectly described by the Hartree product wave function. By replacing the Hartree product with a single Slater determinant, the Hartree–Fock method enforces the antisymmetry of the electronic wave function and ensures compliance with the Pauli exclusion principle [7, 8]

$$\psi_{\mathrm{HF}}(r_1, r_2, ..., r_N) = \\ = \frac{1}{\sqrt{N!}} \begin{bmatrix} \Phi_1(x_1) & \Phi_1(x_2) & \cdots & \Phi_1(x_N) \\ \Phi_2(x_1) & \Phi_2(x_2) & \cdots & \Phi_2(x_N) \\ \vdots & \vdots & & \vdots \\ \Phi_N(x_1) & \Phi_N(x_2) & \cdots & \Phi_N(x_N) \end{bmatrix}, \tag{4}$$

where $\frac{1}{\sqrt{N!}}$ is the normalization of the wave function. The functions $\Phi_i(x_{ij})$ are spin orbitals defined as products of spatial orbitals and spin functions, i.e., $\Phi_i(x_{ij}) = \varphi_i(r)\alpha$ or $\varphi_i(r)\beta$. In this case, the variables x_i include the spatial coordinates and the spin coordinate of the electron. Since exchanging any pair of particles is equivalent to changing two columns, thereby changing the sign of the determinant, it is clear that the wave function ψ_{HF} in Eq. (4) is antisymmetric. In addition, two rows of the Slater determinant are identical according to the Pauli exclusion principle, and if any two particles is in the same single-particle state, the determinant is zero [9].

Froese–Fischer developed computational techniques for the Hartree–Fock atomic equations. The current review articles provide a comprehensive explanation of the various methods developed in this area and a summary of their uses [10, 11].

Q.S. Al-Khafaji, and A.S. Majali (2019) [12] using the Hartree–Fock (HF) wave function investigated various physical properties and 1s and 2s energies of negative ions in the ground state (Li^{-1}, B^{-1}, C^{-1}, N^{-1}, O^{-1}, and F^{-1}) with atomic numbers ($Z = 3$ to 9) and the first and second excited states of (B^{-1}, C^{-1}, and N^{-1}) where ($Z = 5$ to 7). Since most of the previous research focused on determining the energies and examining the atomic properties of atoms and positive ions, this type of work is relatively rare. Therefore, the aim of our study was to investigate the energies of negative ions.

2. Theory

Hartree–Fock theory stands out as one of the more straightforward yet powerful methods for tackling the intricate maze of many-electron systems. Its reach extends widely within the realm of quantum mechanics, finding utility across a spectrum of fields – think atomic structures, molecular interactions, and the dense fabric of solid-state physics, all the way through to the nuances of nuclear interactions and elementary particle fields. At its core, this method hinges on two key ideas: the central field approximation and the variation principle. Now, let's break that down a bit. The central field approximation paints a picture where electrons behave like solitary wanderers, moving independently within an average field generated by the nucleus, while also assuming that this average potential is neatly spherical. It's a bit like imagining a bustling city where each person walks their own path, but there's a common background vibe influencing them all. Merging this approximation with the variation principle, we arrive at the restricted Hartree–Fock equations, determine the spin orbitals of the system, from which the one-particle radial density distribution $D(r_1)$ can subsequently be constructed [10, 12].

But why is $D(r_1)$ such a big deal? Think of it as a map for understanding the electrons nestled within an atom! This crucial distribution reveals the likelihood of spotting electrons in each shell around the nucleus. In essence, it sketches out how one electron is likely to spread itself across the different shells, serving as a foundation for further explorations into the electronic landscape of atoms [13].

2.1. Radial density distribution function of a single-particle $D(r_1)$

The probability of finding electrons in each electron shell is given by the single-particle radial density distribution function $D(r_1)$, which is defined as follows and is necessary to search for electrons in the ion [13, 14]:

$$D\left(r_1\right)=\int\limits_0^{\infty} D\left(r_1, r_2\right) d r_2. \tag{5}$$

2.2. Single-particle expectation value $\langle r_1^n \rangle$

The following formula describes the radial probability density of an electron and the probability of finding it at a particular distance from the nucleus [14, 15]

$$\langle r_1^n \rangle=\int\limits_0^{\infty} D\left(r_1\right) r_1^n d r_1. \tag{6}$$

2.3. The distribution function of electrons $f(r_{12})$

The electron distribution function describes the probability of finding two electrons separated by r_{12} [16, 17]

$$f_{ij}\left(r_{12}\right)=\int \Gamma_{ij}\left(r_1, r_2\right) d r_1 d r_2. \tag{7}$$

Here, the indices (i, j) label the two electrons (or spin orbitals) under consideration.

2.4. Two electrons expectation values $\langle r_{12}^n \rangle$

The following equation represents the expected value of the distance between two electrons [14]:

$$\langle r_{12}^n \rangle=\int\limits_0^{\infty} f\left(r_{12}\right) r_{12}^n d r_{12}. \tag{8}$$

2.5. Standard deviation values $\Delta r_1, \Delta r_{12}$

According to the following equations, the "standard deviation" is the extent to which the single-electron distance and the distance between two electrons differ from their expected values [18]

$$\Delta r_1 \;=\sqrt{\langle r_1^2 \rangle-\langle r_1 \rangle^2}, \tag{9}$$

$$\Delta r_{12}=\sqrt{\langle r_{12}^2 \rangle-\langle r_{12} \rangle^2}. \tag{10}$$

2.6. The energy expectation value $\langle E \rangle$

According to the virial theorem for Coulombic systems, the expectation values of the kinetic and potential energies satisfy the relation [19–21]

$$\langle T \rangle=-\frac{\langle V \rangle}{2}, \tag{11}$$

$$\langle V \rangle=Z\left\langle\frac{1}{r_1}\right\rangle+\left\langle\frac{1}{r_{12}}\right\rangle. \tag{12}$$

3. Results

Using the equations related to the desired quantities, the calculations were implemented in Mathcad 2014 to obtain the results, which were subsequently documented in the tables below, and the relationship of the data was plotted.

Table 1 shows the relationship between the maximum electron presence values $D_{\max}(r_1)$ and the corresponding position values r_1. Table 2 shows the expected electron distances $\langle r_1^n \rangle$ from the nucleus and their standard deviations Δr_1 for different values of

Table 1. **Hartree–Fock wave function values for positions and maximum values of $D(r_1)$ for subshells in a.u.**

Ions	Atomic number	Shell	Peak	r_1	$D_{\max}(r_1)$
S^{-1}	16	2p	Peak1	0.32700	2.11329
		3p	Peak1	0.26550	0.082334
			Peak2	1.67500	0.46738
Cl^{-1}	17	2p	Peak1	0.30330	2.30580
		3p	Peak1	0.24400	0.10095
			Peak2	1.47930	0.53973
K^{-1}	19	2p	Peak1	0.26390	2.68880
		3p	Peak1	0.21000	0.17399
			Peak2	1.16300	0.79510
Sc^{-1}	21	2p	Peak1	0.23360	3.07260
		3p	Peak1	0.18460	0.23289
			Peak2	0.97750	0.97734

n, which is an integer. Table 3 shows the relationship between the maximum values of the interatomic distribution function $f_{\max}(r_{12})$ and their corresponding location values r_{12}. Table 4 shows the expected interatomic distance values $\langle r_{12}^n \rangle$ and their standard deviations Δr_1 for different values of n, which is an integer.

Table 2. **Expectation values $\langle r_1^n \rangle$ and standard deviation where $-2 \le n \le 2$ for subshells in a.u.**

Ions	Shells	$\langle r_1^{-2} \rangle$	$\langle r_1^{-1} \rangle$	$\langle r_1^{+1} \rangle$	$\langle r_1^{+2} \rangle$	Δr_1
S^{-1}	2p	12.20200	2.95400	0.44100	0.24200	0.21818
	3p	0.80200	0.59400	2.32100	6.70900	1.15003
Cl^{-1}	2p	14.28700	3.20300	0.40500	0.20400	0.19881
	3p	1.04300	0.68000	2.02800	5.09700	0.99235
K^{-1}	2p	18.92600	3.69700	0.34900	0.15100	0.16942
	3p	1.94700	0.93900	1.43700	2.44000	0.61277
Sc^{-1}	2p	24.23100	4.19200	0.30700	0.11600	0.14755
	3p	2.86700	1.14200	1.18700	1.65900	0.50094

Table 3. **Hartree–Fock wave function values for r_{12} and maximum values of $f_{\max}(r_{12})$ for subshells in a.u.**

Ions	Atomic number	Shell	r_{12}	$f_{\max}$
S^{-1}	16	2p	0.51800	1.45460
		3p	2.73800	0.28381
Cl^{-1}	17	2p	0.47800	1.58620
		3p	2.41200	0.32591
K^{-1}	19	2p	0.41400	1.84670
		3p	1.81700	0.46941
Sc^{-1}	21	2p	0.36500	2.10700
		3p	1.51300	0.56861

Table 4. **Expectation values $\langle r_{12}^n \rangle$ and standard deviation where $-2 \le n \le 2$ for subshells in a.u.**

Ions	Shells	$\langle r_1^{-2} \rangle$	$\langle r_1^{-1} \rangle$	$\langle r_1^{+1} \rangle$	$\langle r_1^{+2} \rangle$	Δr_1
S^{-1}	2p	6.98305	2.07865	0.63115	0.48430	0.29317
	3p	0.25687	0.39610	3.31475	13.41832	1.55909
Cl^{-1}	2p	8.23654	2.25937	0.57961	0.40772	0.26789
	3p	0.33513	0.45263	2.89318	10.19446	1.35055
K^{-1}	2p	11.03341	2.61806	0.49909	0.30162	0.22919
	3p	0.64211	0.63040	2.02920	4.87971	0.87295
Sc^{-1}	2p	14.24415	2.97702	0.43813	0.23210	0.20035
	3p	0.94176	0.76251	1.67511	3.31854	0.71591

Table 5 shows the values of the attractive energy $-\langle V_{en} \rangle$ between the electron and the nucleus, the repulsive energy $\langle V_{ee} \rangle$ between the electrons, the total potential energy $-\langle V_T \rangle$, the kinetic energy $\langle T \rangle$ and the total energy (Hartree–Fock energy) $-\langle E_T \rangle$ for each shell.

Figure 1 shows the relationship between the change in the electron distribution function and the position values of the studied elements, while Fig. 2 shows the relationship between the interatomic distribution function and the interatomic distance values.

4. Discussion

By applying the above equations, the results were systematically tabulated and plotted. Table 1 and Fig. 1 present several results indicating that the probability of detecting an electron increases as the distance between the electron and the nucleus decreases and the maximum values of $D(r_1)$ increase with increasing r_1. Moreover, we note that these peaks are concentrated in the vicinity of the nucleus, where we also observe the maximum probability density distribution function for the systems under study. For the negative ion systems under study, the maximum values of the single-particle radial density distribution function $D(r_1)$ increase with increasing atomic number Z for each shell (2p) and (3p). This increase in values is due to the increasing force of attraction between the nucleus and the electrons with increasing atomic number. It is also important to note that in Fig. 1, as the positions of the extreme values of r_1 decrease, the probability of finding an electron is zero when the distance is zero. This means that the electron cannot be inside the nucleus, but when the dis-

Table 5. **Expectation values for all attraction, repulsion potential, kinetic and total energy for subshells in a.u.**

Ions	Shells	$-\langle V_{en} \rangle$	$t\langle V_{ee} \rangle$	$\langle V_T \rangle$	$\langle T \rangle$	$-\langle E_T \rangle$
S^{-1}	2p	94.28000	2.07865	92.44935	46.22468	46.22468
	3p	19.00800	0.39610	18.61190	9.30595	9.30595
Cl^{-1}	2p	108.90200	2.25937	106.64263	53.32131	53.32131
	3p	23.12000	0.45263	22.66737	11.33369	11.33369
K^{-1}	2p	140.48600	2.61806	137.86794	68.93397	68.93397
	3p	35.68200	0.63040	35.05160	17.52580	17.52580
Sc^{-1}	2p	176.06400	2.97702	173.08698	86.54349	86.54349
	3p	47.96400	0.76251	47.20149	23.60074	23.60074

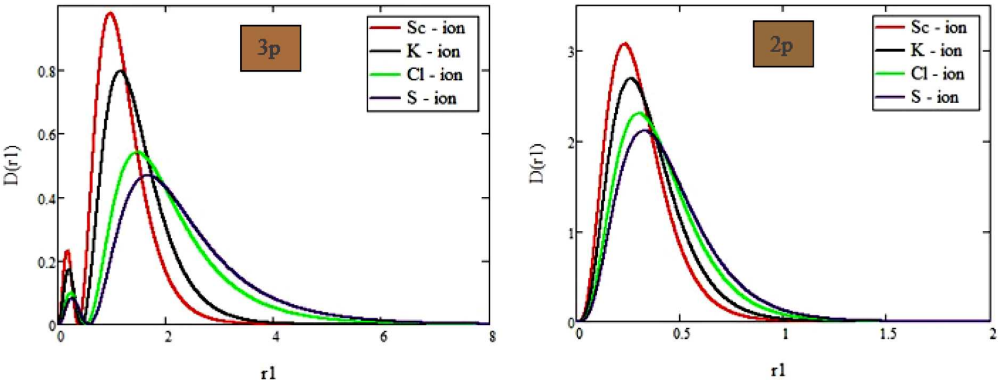

Fig. 1. Relationship between the location r_1 and the one particle radial density distribution function $D(r_1)$

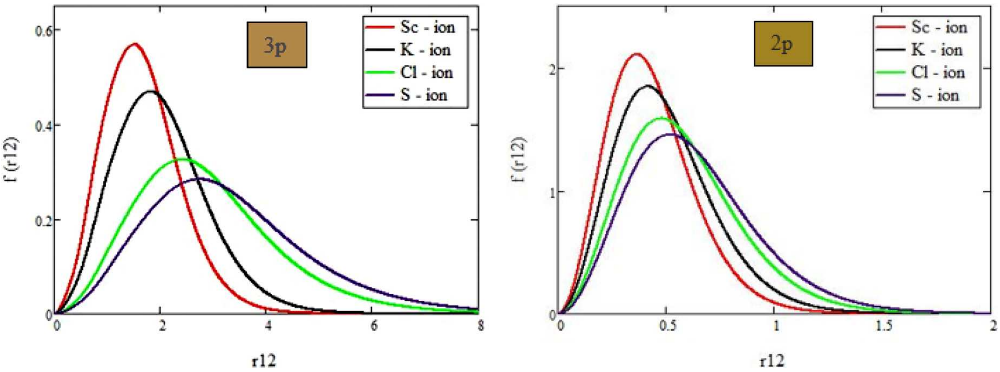

Fig. 2. The relationship between r_{12} and the inter-particle distribution function

tance is far the probability of finding an electron is zero, which means that the electron cannot be outside the atom.

According to Fig. 1, there is only one peak representing the probability of finding an electron in the 2p shell and two peaks reflecting the probability of finding an electron in the 3p shell. The second peak shows the probability of finding an electron in the 3p shell, while the first peak depicts an electron that can penetrate the 2p shell or remain in it briefly.

Table 3 and Fig. 2 show that the effect of the nuclear attractive force leads to an increase in the probability of the distribution function $f(r_{12})$ between particles with increasing atomic number Z. We notice from Table 3 that the probability of finding two electrons in the 2p shell separated by a distance r_{12} at the same time is higher than the probability of that in the 3p shell. Because the 2p shell is closer to the nucleus than the 3p shell, the distance between the two electrons becomes smaller, which increases the probability of finding the two electrons.

For all shells (2p and 3p), Tables 2 and 4 show that when n is negative, the expected values ($\langle r_1^n \rangle$ and $\langle r_{12}^n \rangle$) for the negative ions in question grow with increasing atomic numbers. Conversely, when n is positive, the reverse happens. As the atomic number of all shells increases, the standard deviations (Δr_1 and Δr_{12}) obviously decrease.

According to Table 5, the calculated values of all energies ($-\langle V_{en} \rangle$, $\langle V_{ee} \rangle$, $-\langle V_T \rangle$, $\langle T \rangle$, and $-\langle E_T \rangle$) increase with increasing atomic number for all studied negative ion shells. The table also shows that the binding energy between the electrons and the nucleus increases as the distance between the electrons decreases, which leads to an increase in the force of repulsion between the electrons. Since other energies depend on ($-\langle V_{en} \rangle$, $\langle V_{ee} \rangle$), this results in an increase in the remaining energy terms.

5. Conclusion

According to the present study, the conclusions of the HF method for all shells under investigation is that with increasing atomic number, the maximum values of the single-particle radial density distribution function $D(r_1)$ and the interparticle distribution function $f(r_{12})$ increase, and their positions decrease. As the atomic number increases, the values $\langle r_1^n \rangle$ and $\langle r_{12}^n \rangle$ decrease for positive n values, while they increase for negative n values. In this regime, the standard deviations (Δr_1 and Δr_{12}) decrease as the atomic number increases. Within the Hartree–Fock approximation, the calculated expectation values of the kinetic, potential, and total energies increase with increasing atomic number for the considered negative ions. These estimates and Hartree–Fock calculations are used to provide a theoretical database for this set of systems for future use by researchers.

1. G. Fano, S.M. Blinder. *Twenty-First Century Quantum Mechanics: Hilbert Space to Quantum Computers* (Springer International Publishing, 2017).
2. A. Sharma. *A Textbook on Modern Quantum Mechanics* (CRC Press, Boca Raton, 2021) [ISBN: 978-1-003-15445-7].
3. M. Breinig. Schrödinger equation. In: *Compendium of Quantum Physics*. Editet by D. Greenberger, K. Hentschel, F. Weinert (Springer, 2009) [ISBN: 978-3-540-70622-9].
4. J.G. Lietz, S. Novario, G.R. Jansen, G. Hagen, M. Hjorth-Jensen. Computational nuclear physics and post Hartree-Fock methods. In: *An Advanced Course in Computational Nuclear Physics*. Edited by M. Hjorth-Jensen, M. Lombardo, U. van Kolck (Lecture Notes in Physics, vol 936 (Springer, 2017) [ISBN: 978-3-319-53335-3].
5. M.J. Al-Sharaa, M.A. Mahmood, N.C. Madhkoor, K.H. Al-Bayati. Energy calculation for beryllium atom in different excited states (1s^2 2s 3s), (1s 2s^2 3s) and (1s 2s 3s^2). *AIP Conf. Proc.* **1888** (1), 020013 (2017).
6. A.F. Al-Assady, Q.S. Al-Khafaji. Study of atomic properties for subshells of the systems with $Z = 12$–16 using the Hartree–Fock approximation. *IOP Conf. Ser.: Mater. Sci. Eng.* **928** (7), 072107 (2020).
7. D.R. Hartree. *The Calculation of Atomic Structures* (John Wiley and Sons, 1957) [ISBN: 978-3-319-53335-3].
8. M.J. AL-Sharaa. Evaluation and comparison of the configuration potential energy calculation for be-atom in position space. *Misan J. Acad. Stud.* **16** (32), 202 (2017).
9. M. Cini. Systems of particles. In: *Elements of Classical and Quantum Physics* (Springer, 2018).
10. A.W. King, L.C. Rhodes, H. Cox. Inner and outer radial density functions in correlated two-electron systems. *Phys. Rev. A* **93** (2), 022509 (2016).
11. H. Yserentant. On the complexity of the electronic Schrödinger equation. Preprint, **50**, DFG-SPP 1324, June 2010.
12. E.S. Majali, Q.S. AL-Khafaji. Calculation of the energies of negative ion of (B^{-1}, C^{-1} and N^{-1}) for ground and excited states. *Theor. Appl. Sci.* **10**, 536 (2019).
13. S.B. Doma, G.D. Roston, M.F. Ahmed. Application of the Variational Monte Carlo method to the three electron Coulomb and harmonium systems. *Int. J. Sci. Res. Phys. Appl. Sci.* **10** (4), 01 (2022).
14. K.E. Banyard, G.J. Seddon. Coulomb holes and expectation values. I. Explicitly correlated wavefunctions. *J. Chem. Phys.* **58**, 3, 1132 (1973).
15. M.H. AL-Quraishi, A.F. Shamkhi, Q.S. AL-Khafaji, A.K. Shaymaa, N.H. Alie. Calculation of the correlation energy of three electron systems of 20 to 25 electrons. *J. Iraqi Al-Khwarizmi* **7** (2), 34 (2023).
16. Q.S. Al-Khafaji, S.A.K. Al-Shebly, H.H.J. Bilal, N.H. Ali. Calculating the energy of B_2^+-ion using division technique. *J. Adv. Phys.* **5** (4), 364 (2016).
17. W.A. Hussein, M.J. AL-Sharaa. Calculation of the atomic properties of excited states for B-atom using Hartree–Fock approximation. *J. Adv. Phys.* **11** (8), 3951 (2016).
18. M.H. AL-Quraishi, Q.S. AL-Khafaji. Evaluation of the Hartree–Fock energy of four electron systems. *NeuroQuantology* **20**(6), 4115 (2022).
19. K.S. AL-Khafiji, A.M. Selman, S.A.K. Al-Shebly. Calculation of the standard deviation and nuclear magnetic shielding constant for lithium atom. *J. Kerbala Univ.* **6** (2), 107 (2008).
20. T. Tsuneda. Hartree–Fock Method. In: *Density Functional Theory in Quantum Chemistry* (Springer, 2014).
21. S.L. Saito. Hartree–Fock–Roothaan energies and expectation values for the neutral atoms He to Uuo: The B-spline expansion method. *At. Data Nucl. Data Tables* **95** (6), 836 (2009).

Received 15.02.25

М.Дж. Аль-Шараа, Х.Ю.Я. Аль-Казраджі,
К.Ш. Аль Хафаджі, Ш.А. Кадхім

РОЗРАХУНОК ЕНЕРГІЙ ХАРТРІ–ФОКА ОБОЛОНОК p-ТИПУ ДЕЯКИХ НЕГАТИВНИХ ІОНІВ

Розраховано енергії підоболонок (2p, 3p) та деякі важливі атомні властивості низки іонів (S$^{(-1)}$, Cl$^{(-1)}$, K$^{(-1)}$ та Sc$^{(-1)}$) за допомогою методу Хартрі–Фока. Енергії оцінено для атомних номерів $16 \leq Z < 21$. Дослідження показало, що оцінки, використані для розрахунку атомних властивостей за допомогою цього методу, були точними. Було досліджено функції $D(r_1)$ та $f(r_{12})$, які, відповідно, описують ймовірність знаходження одного електрона та двох електронів, розділених відстанню r_{12}, а також досліджено ймовірності Хартрі–Фока $\langle r_{12}^n \rangle$, $\langle r_1^n \rangle$, де n – значення від –2 до 2. Було розраховано значення енергії $\langle E_{\mathrm{HF}} \rangle$, $\langle V_T \rangle$, $\langle V_{en} \rangle$, $\langle V_{ee} \rangle$ та $\langle T \rangle$. Можна зробити висновок, що збільшення атомного номера приводить до збільшення всіх досліджуваних енергій розглянутих елементів. Усі функції були стандартними. Для програмування рівнянь використовувався додаток Mathcad 2014. Щодо обчислень, то всі вони були виконані в атомних одиницях (а.о.).

Ключові слова: рівняння Шредінгера, атомні властивості, негативний іон, енергії Хартрі–Фока.